Rate Processes in Cycling a Reversible Gas-Solid Reaction

M. A. STANISH and
D. D. PERLMUTTER

Department of Chemical Engineering
University of Pennsylvania
Philadelphia, PA 19104

Rate studies are reported of the effect of rehydration-dehydration cycling on the vapor hydration behavior of solid K_2CO_3. Isothermal rate data were obtained at different temperatures and water vapor pressures for the reaction of narrowly-sized anhydrous particles. Effects of different particle preparation histories on the rehydration rate were investigated and correlations of rate with particle pore structure explored. Rehydration rates of dehydrated $K_2CO_3 \cdot 3/2H_2O$ were found to depend on the conditions of the prior dehydration. Rehydration is comparatively very slow at relative pressures below $P/P_{eq} \simeq 1.5$; rates increase linearly with pressure above $P/P_{eq} \simeq 3$. Hydration rates of K_2CO_3 particles obtained as anhydrous are substantially slower than those of identically-sized crystals produced by prior dehydration of $K_2CO_3 \cdot 3/2H_2O$; after one rehydration-dehydration cycle, rehydration rates are increased by as much as two orders of magnitude and this distinction between sources virtually disappears. Diffusional resistances based on calculated water vapor diffusivities are qualitatively consistent with the observed effects of cycling but do not by themselves account fully for the observations.

SCOPE

The hydration reaction of K_2CO_3 with water vapor is of interest from two different perspectives. First, this system serves as a convenient prototype for the study of kinetics in reversible gas-solid reactions of inorganic salts, a topic of recognized industrial importance. Second, water and K_2CO_3 were shown (Stanish and Perlmutter, 1981) to hold significant promise as a refrigerant-absorbent pair in a low-temperature heat pump cycle. Since little information is available concerning the kinetics of hydration and dehydration in the water-K_2CO_3 system, an experimental study of these phenomena is needed to more accurately determine the feasibility and potential of a real K_2CO_3-based heat pump device.

The objectives of this study were to identify the variables that are most important in determining the rehydration rate of K_2CO_3 particles and to quantify their effects. This investigation includes evaluation of the importance of the source of the solid and the method of preparation in determining the rate of rehydration. In addition, the effect of water vapor pressure on reaction rate is quantified. Finally, changes in rehydration rate with rehydration-dehydration cycling are explored, and correlations are sought with the differences in particle pore structure revealed by mercury intrusion porosimetry data. The behavior of this system is compared to that reported for the reversible decomposition of Ag_2CO_3.

CONCLUSIONS AND SIGNIFICANCE

The rate of rehydration of dehydrated $K_2CO_3 \cdot 3/2H_2O$ crystals is affected by the prior dehydration conditions; samples that were dehydrated more rapidly (at higher temperature and/or lower pressure) were subsequently found to rehydrate more rapidly as well. Slow rehydration and the appearance of induction and acceleration in rehydration conversion time curves were characteristics of $K_2CO_3 \cdot 3/2H_2O$ dehydrated at relatively high water vapor pressures and/or rehydrated at relatively low pressures. The effect of water vapor pressure on rehydration rate is not first order; rates are extremely slow at pressures close to the equilibrium value ($P/P_{eq} < 1.5$) but rise gradually with increasing pressure and become linear in pressure for $P/P_{eq} > 3$. Qualitatively, this behavior mirrors what was previously observed for the dehydration of $K_2CO_3 \cdot 3/2H_2O$ (Stanish and Perlmutter, 1982).

The effect of cycling is to increase the rate of rehydration. For $K_2CO_3 \cdot 3/2H_2O$ crystals, the rate enhancement after the first cycle is relatively small if the dehydration step is carried out in vacuum but is more significant for dehydration in water vapor. For K_2CO_3 particles obtained in anhydrous form the rate change due to the first cycle spans approximately two orders of magnitude; after one cycle, particles from this source rehydrate at rates similar to those of dehydrated $K_2CO_3 \cdot 3/2H_2O$ crystals.

Particle diffusivities calculated on the basis of measured pore volume distributions were found to decrease with rehydration conversion to a greater degree in the less reactive samples. Thus, restricted mass transfer within the solid particles appears to be a likely explanation for the observed attenuation in rehydration rates. However, transport-related effects cannot fully account for other aspects of hydration behavior that are associated with cycling, and other mechanistic interpretations are needed to explain the reported observations.

The results reported here have a mixed impact on the perceived potential of the water vapor-K_2CO_3 system for utilization in heat pump cycles. Rehydration rates were demonstrated to increase substantially with cycling; such behavior is certain to be an advantage in any heat pump application. On the other hand, low rehydration rates at small relative pressures ($1.0 < P/P_{eq} < 1.5$) are unfavorable. Further tests appear to be warranted.

INTRODUCTION

Interest in salt hydrates arises in part from the recognition of their potential application in domestic solar heating and cooling applications (Grodzka, 1975). In particular, the use of solid inorganic salt hydrates as absorbents in heat pump cycles was shown (Stanish and Perlmutter, 1981) to offer significant improvements in performance efficiencies compared to those of cycles using

previously-proposed solid or liquid absorbents. Little is known, however, about vapor rehydration of solid inorganic salts, nor are the effects of cycling on these reactions well defined.

Bielanski and Tompkins (1950) studied the rehydration of dehydrated alum crystals. The hydration was fully reversible and the conversion was proportional to the square-root of time when less than about 6 mol of water were absorbed per mole of salt. If the salt was allowed to absorb more than this amount of water, it was transformed to a state with a glassy appearance and the additional water became very difficult to remove.

The rehydration of manganous formate produced from the vacuum dehydration of the dihydrate has been studied in detail by Eckhardt et al. (1971). This material was found to rehydrate smoothly and completely to the dihydrate composition, unlike nickel and manganous oxalates, which rehydrate only very slowly after an initial, rapid reaction. For manganous formate, a plot of percent rehydration against the square-root of time yielded two linear regions. Dehydrated single crystals and crystalline powder rehydrated at similar rates in contrast to the initial dehydration (Eckhardt and Flanagan, 1964), in which the powder reacted at considerably higher rates. The rehydration did not occur below a supersaturation ratio of about 10; above this level the rate increased markedly with pressure.

Ball and Norwood (1973) investigated the vapor rehydration of hexagonal $CaSO_4$ produced from the dehydration of the dihydrate and found that the conversion was also best described by a square-root-of-time dependence. The derived rate constants were interpreted to show that rehydration only occurs on surfaces covered by at least a monolayer of adsorbed water.

The effect of the initial dehydration conditions on the subsequent rehydration behavior appears to depend on the individual salt. For example, Eckhardt et al. reported that the rehydration behavior of manganous formate was not affected by differences in the temperature of the previous vacuum dehydration within the range 298 to 373 K. Similarly, Ball and Norwood observed no differences in the behavior of anhydrous $CaSO_4$ that was produced at unspecified temperatures and partial water vapor pressures. On the other hand, Triollier and Guilhot (1976) concluded that only gypsum ($CaSO_4 \cdot 2H_2O$) dehydrated in a vacuum or in a very low water vapor pressure (<1.3 kPa) was likely to rehydrate. Indeed, they observed marked differences in the rehydration behavior of gypsum dehydrated at 403 K in a vacuum or under 1.3 kPa water vapor. Likewise, Flanagan (1959) discovered that samples of lead styphnate dehydrated in vacuum rehydrated six times as fast as did samples dehydrated under 100 Pa water vapor.

Information concerning the effect of cycling is extremely rare. As part of their work on the dehydration of copper sulfate pentahydrate, Hume and Colvin (1932) investigated the effect of rehydration on the dehydration rates. The complete rehydration of the monohydrate produced a pentahydrate in a much finer state of division than that of the original crystals. The actual size depended on the degree of aggregation attained during rehydration; this in turn was found to depend on such factors as the relative rate and total time of the rehydration process. The subsequent dehydration rate decreased with increasing aggregation. Eckhardt et al. reported that the rate of manganous formate dihydrate dehydration increased with successive cycles, while the rate of rehydration decreased with cycling. Both rates eventually became reproducible after an unspecified number of cycles. Flanagan (1966) reported that both the hydration and dehydration rates of lead styphnate were enhanced by cycling, even up to 30 cycles.

EXPERIMENTAL PROCEDURES

Experiments were performed with either J. T. Baker Chemical Co. reagent grade $K_2CO_3 \cdot 3/2H_2O$ or anhydrous K_2CO_3, separated by sieving into relatively narrow particle size ranges. The rehydration behavior of samples weighing 5 to 10 mg was observed in a Dupont model 951 Thermogravimetric Analyzer (TGA) connected to a vacuum pump and to a water vapor pressure control system. Sample temperature was maintained by the TGA furnace and measured by a chromel-alumel thermocouple

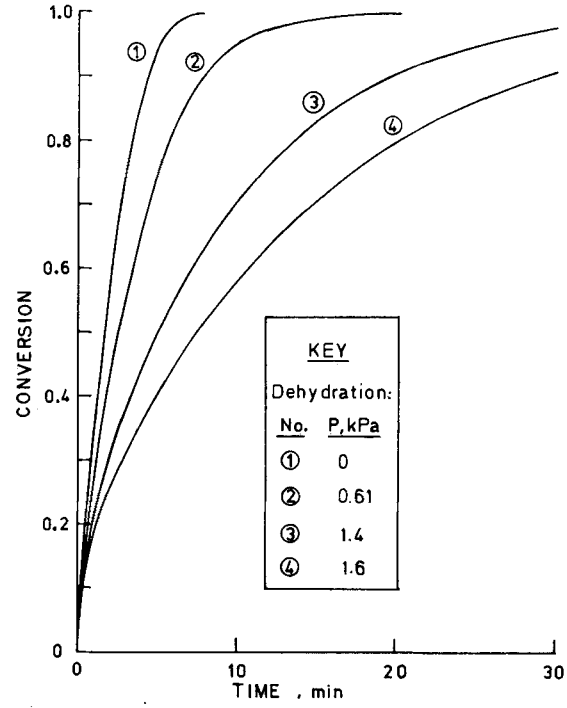

Figure 1(a). Hydration at T = 305.5 K, P = 1.3 kPa of K_2CO_3 particles prepared from 300–354 μm (−45 + 50 mesh) $K_2CO_3 \cdot 3/2H_2O$ crystals at 348 K and different pressures.

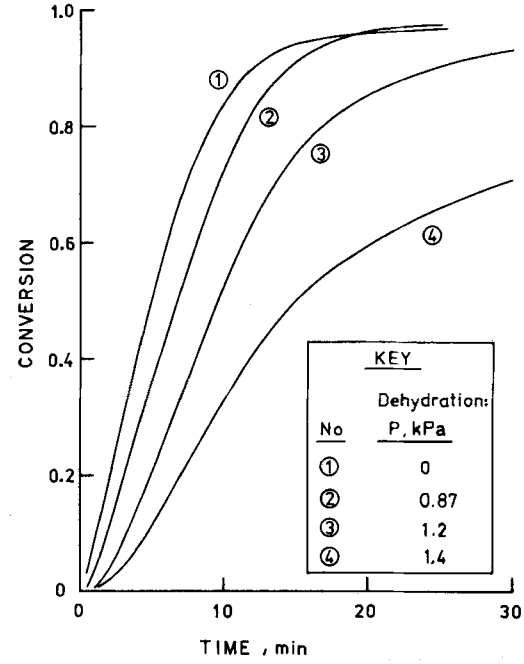

Figure 1(b). Hydration at T = 333 K, P = 2.3 kPa of K_2CO_3 particles prepared from 300–354 μm (−45 + 50 mesh) $K_2CO_3 \cdot 3/2H_2O$ crystals at 353 K and different pressures.

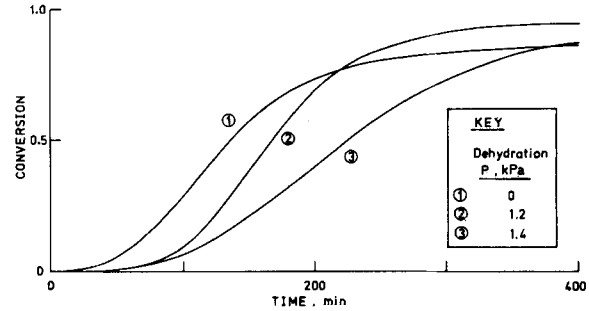

Figure 1(c). Hydration at T = 333 K, P = 1.6 kPa of K_2CO_3 particles prepared from 300–354 μm (−45 + 50 mesh) $K_2CO_3 \cdot 3/2H_2O$ crystals at 353 K and different pressures.

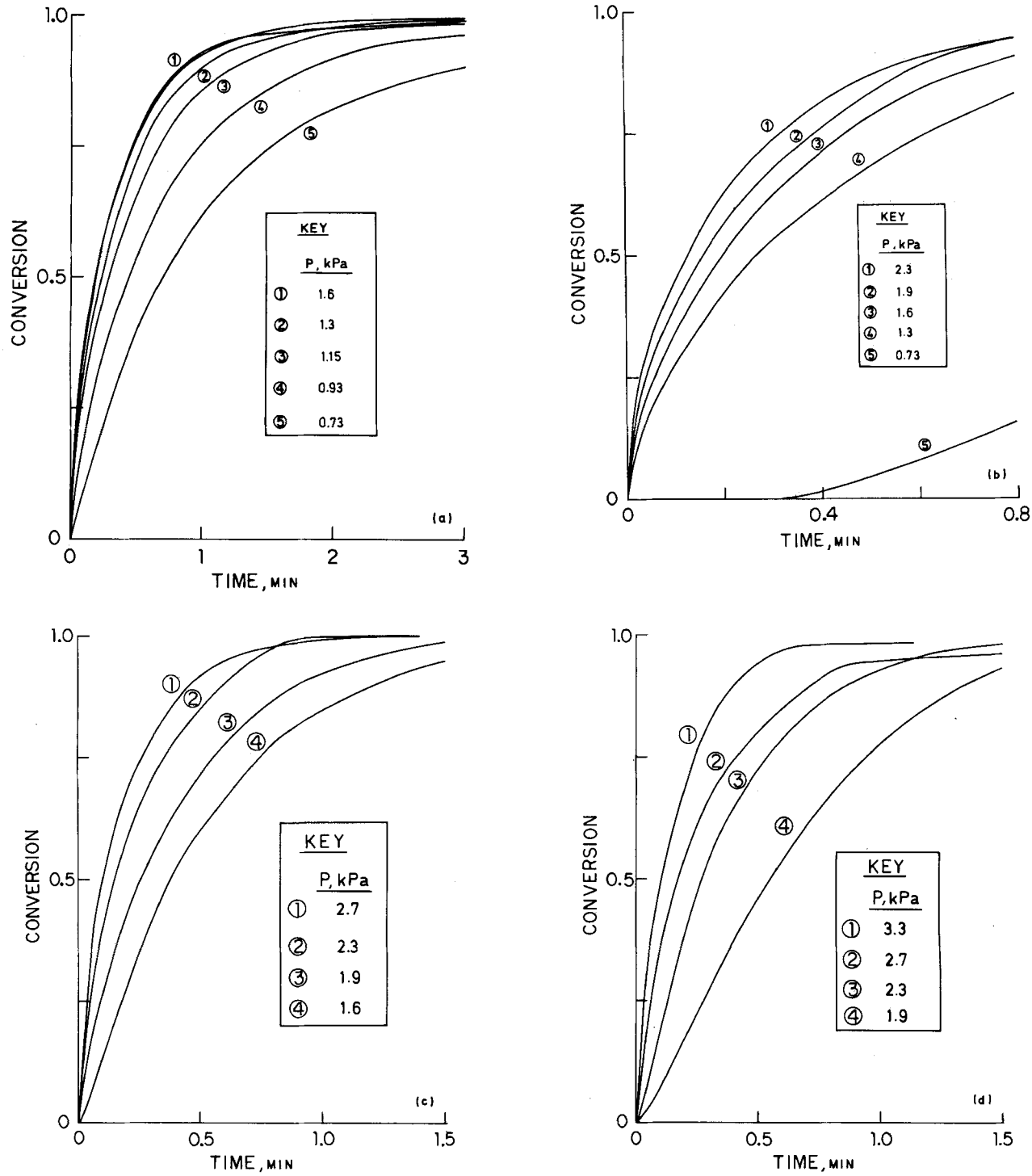

Figure 2. Effect of pressure on the hydration $K_2CO_3 + 3/2H_2O \rightarrow K_2CO_3 \cdot 3/2H_2O$ at different temperatures. Anhydride prepared from 75–90 μm (−170 + 200 mesh) $K_2CO_3 \cdot 3/2H_2O$ crystals at $T = 360$ K, 1.3 kPa. (a) $T = 305.5$ K ($P_{eq} = 110$ Pa); (b) $T = 312$ K ($P_{eq} = 200$ Pa); (c) $T = 319.5$ K ($P_{eq} = 360$ Pa); (d) $T = 327$ K ($P_{eq} = 640$ Pa).

placed adjacent to the sample pan. The output of this thermocouple and the weight of the salt sample were recorded as a function of time. Pore size distribution data were measured with a Micromeritics model 915 mercury intrusion porosimeter.

Samples of $K_2CO_3 \cdot 3/2H_2O$ crystals were first dehydrated at the designated conditions using previously-described techniques (Stanish and Perlmutter, 1982). Samples of anhydrous K_2CO_3 were first pretreated in a vacuum at 353 K to remove any absorbed water. In either case, the dried sample was cooled under a vacuum to the temperature of interest. After several minutes of equilibration, the balance housing was joined to a flask of distilled water maintained at the saturation temperature of the water vapor pressure of interest. The pressure in the housing thus rose immediately to this preselected level, initiating the isothermal, isobaric rehydration.

RESULTS AND DISCUSSION

Under the optical microscope, the rehydration of anhydrous K_2CO_3 produced no obvious change in the solid's appearance. Thus it was not possible *a priori* to specify a likely reaction model and develop the appropriate analytical equation to describe the particle reaction kinetics. Instead, particle hydration experiments were carried out in the TGA balance apparatus to identify the factors that influence the observed hydration rates.

Preliminary Rate Studies

The first variable observed to have an effect on hydration rates

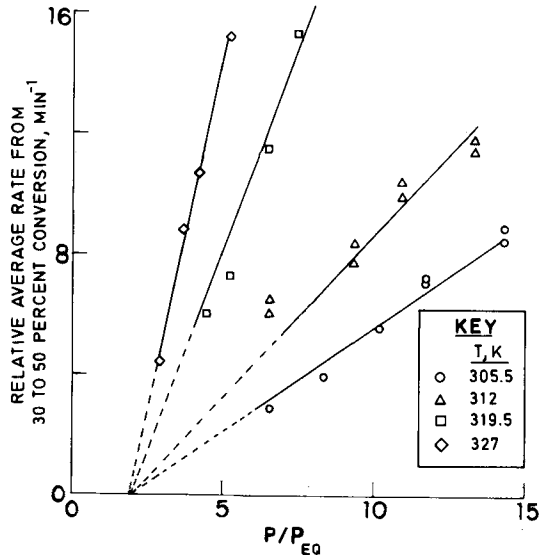

Figure 3. Water vapor pressure dependence of K_2CO_3 hydration rates at conditions far from equilibrium.

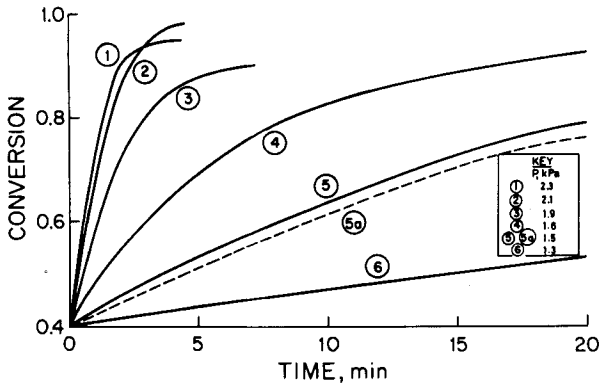

Figure 4. Effect of pressure on K_2CO_3 hydration at $T = 333$ K ($P_{eq} = 1.0$ kPa). Initial conversion ($X < 0.4$) at $P = 2.8$ kPa. Anhydride prepared from 75–90 μm (−175 + 200 mesh) $K_2CO_3 \cdot 3/2H_2O$ crystals at $T = 353$ K in vacuum. (Curves 5 and 5a are replicate experiments indicating the level of reproducibility.)

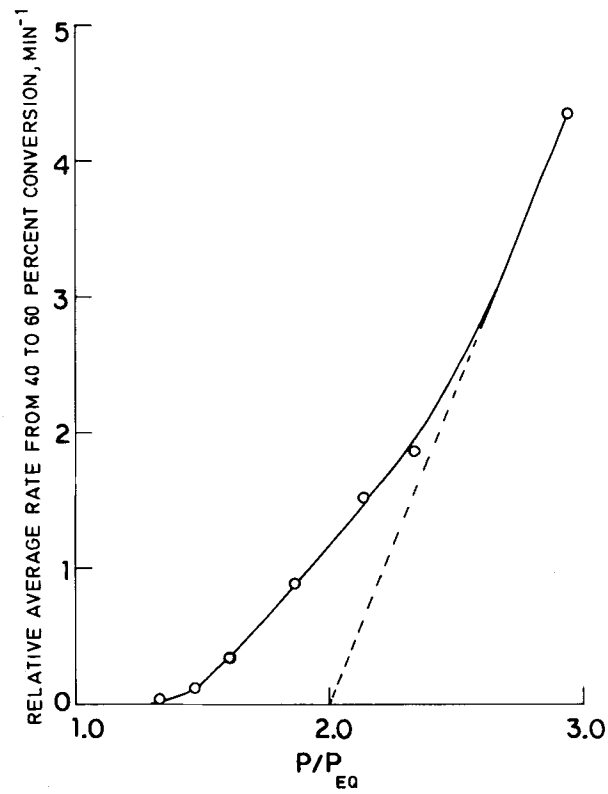

Figure 5. Rate of hydration as a function of pressure (from the data in Figure 4).

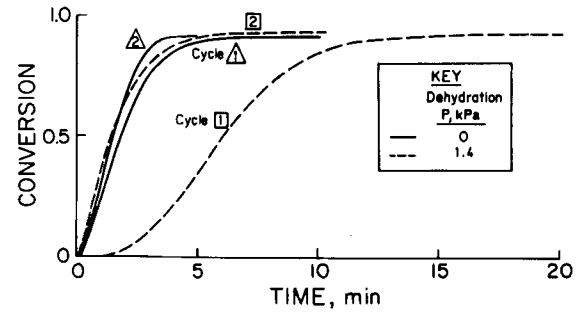

Figure 6. Cyclic rehydration of K_2CO_3 (initially 75–90 μm (−170 + 200 mesh) $K_2CO_3 \cdot 3/2H_2O$ crystals at $T = 333$ K, $P = 2.3$ kPa. Intermediate dehydrations at $T = 353$ K and different pressures.

was that of sample size (weight), presumably due to a resistance to the passage of water vapor through the thicker particle layer of the larger samples. Because of this observation, the samples for all subsequent experiments were spread onto the TGA sample pan as thinly as possible; for particles larger than 300 μm (50 mesh), a monolayer was used. The hydration rate was found to be independent of particle size for particles smaller than 90 μm (170 mesh).

The hydration rate of anhydrous particles obtained by the dehydration of $K_2CO_3 \cdot 3/2H_2O$ crystals was found, however, to depend on the conditions employed for the prior dehydration. As shown in each of the Figures 1(a), (b) and (c), the rate of rehydration is slower for anhydrous material produced by prior dehydration under higher pressures of water vapor. The isothermal hydration conditions are farthest from the equilibrium state (i.e., P/P_{eq} is largest) in Figure 1(a) and are nearest (P/P_{eq} is smallest) in Figure 1(c). In Figures 1(b) and (c), higher water vapor pressure during the preceeding dehydration is seen to bring about increasingly pronounced induction and acceleration in the conversion-time curves for the subsequent rehydration.

Water Vapor Pressure

The results of a series of isothermal, isobaric rehydration experiments on anhydrous particles prepared by identical means are presented in Figure 2, demonstrating that increased vapor pressures of water act to increase reaction rates. This observation may be made quantitative by defining a relative average rate (RAR) as the reciprocal of the time required to react from 30 to 50% conversion. The relative rates obtained in this way are compared in Figure 3 as a function of a reduced pressure based on the vapor pressure of $K_2CO_3 \cdot 3/2H_2O$ at the particular temperature. These rates increase linearly with pressure, but extrapolation of the data predicts that the rate of hydration would vanish not at the equilibrium point, but instead at a pressure about twice as high.

The pressure dependence of the rate of hydration near equilibrium was measured more directly in a different manner. Samples of anhydrous particles prepared in the same way were exposed in the TGA to a high pressure (2.8 kPa) of water vapor at 333 K until they were 30 to 40% hydrated. The pressure was then quickly lowered and held constant at the pressure in interest. The purpose of this procedure was to promote nucleation and to ensure that the initial reaction proceeded in a reproducible manner; in this way the total interfacial area available for rehydration should be the same in each sample and direct rate comparisons can be made. The results of the experiments appear in Figure 4 and the relative rates of hydration between 40 and 60% conversion are compared as a function of reduced pressure in Figure 5. The asymptotic behavior

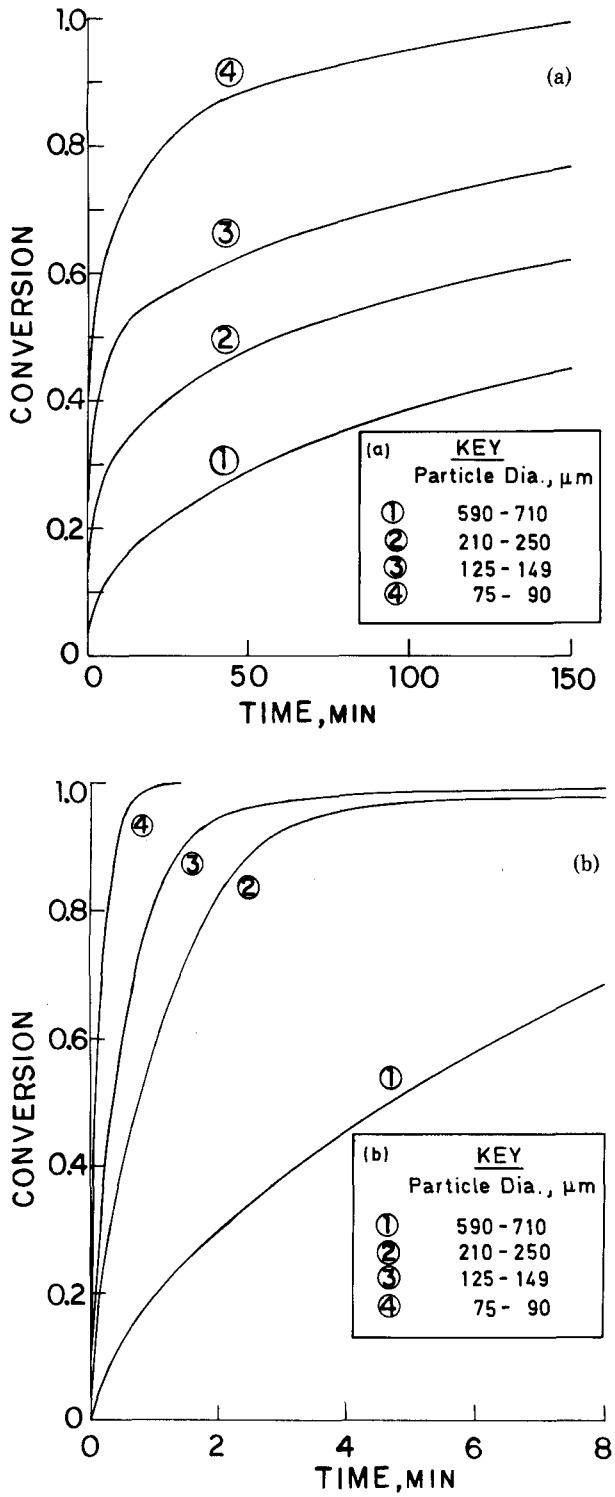

Figure 7. Effect of particle size on the hydration of anhydrous K_2CO_3 at T = 305.5 K, P = 1.3 kPa. (a) First-cycle hydration; (b) Second-cycle hydration; intermediate dehydration at T = 360 K, P = 1.3 kPa.

at pressures far from equilibrium appears to be consistent with the previous measurements at higher pressures (Figure 3); the rate becomes very small at a pressure somewhat removed from the equilibrium point, a dependence qualitatively similar to that discovered for the dehydration reaction (Stanish and Perlmutter, 1982).

Effect of Cycling

The effect of cycling on the rehydration behavior of dehydrated $K_2CO_3 \cdot 3/2H_2O$ crystals is illustrated in Figure 6. When the dehydration was carried out in water vapor, the second cycle produced a significant increase in the rehydration rate and was followed by changes of ever smaller magnitude in succeeding cycles. When the dehydration occurred in a vacuum, the more rapid rate of the first hydration was enhanced to a lesser degree by the second cycle. The end result was that the hydration rate of a cycled hydrate particle was far less dependent on the dehydration conditions than was the hydration rate of the same particle after the initial dehydration.

TABLE 1. EXPERIMENTAL POWDER X-RAY DIFFRACTION DATA FOR DEHYDRATED $K_2CO_3 \cdot 3/2H_2O$

Line No.	Relative Intensity	Measured d-Spacing, Å
1	3	3.338
2	5	2.953
3	10	2.808
5	6	2.609
6	4	2.376
7	1	2.302
8	5	2.100
9	2	1.986
10	1	1.860

The effect of cycling on the rehydration behavior of a sample originally obtained as anhydrous particles is illustrated in Figure 7. The initial hydration was very slow compared to the results in Figure 6; however, the second cycle exhibited a large increase in the rate of rehydration. In fact, these second-cycle rates were very similar to those of dehydrated $K_2CO_3 \cdot 3/2H_2O$ crystals. [Compare for example the data for 75–90 μm (−170+200 mesh) particles in Figures 2(a) and 7(b).]

Solid Structure and Rehydration

In light of the different rehydration rates observed for particles of the same chemical composition, correlations were sought between rehydration behavior and physical properties or particle structure. Powder X-ray diffraction photographs of dehydrated $K_2CO_3 \cdot 3/2H_2O$ and of uncycled anhydrous K_2CO_3 proved to be identical. The measured line spacings and estimated relative intensities of the diffraction patterns given in Table 1 agree well with the known data for crystalline K_2CO_3. Scanning electron micrographs of anhydrous particles before and after one rehydration-dehydration cycle were virtually identical in spite of the very different rehydration rates exhibited by such particles.

It is apparent in Figure 7(a) that the first-cycle rehydration behavior of anhydrous K_2CO_3 particles may be characterized as an initial rapid reaction followed by a period of substantially lower rate in which the reaction slowly approaches completion. The extent of conversion during the initial rapid reaction decreases with increasing particle size, suggesting that transport processes are related to the transition from rapid to slow rates.

This phenomenon was explored via pore structure measurements at different hydration conversions for particles that rehydrate at different rates. The pore volume data for uncycled anhydrous K_2CO_3, which hydrates very slowly after a short initial period of rapid reaction, are shown at different conversion levels in Figure 8. Cumulative pore volume decreases from about 7×10^{-5} m^3/kg K_2CO_3 to less than 3×10^{-5} m^3/kg K_2CO_3 near 80% conversion with an accompanying decrease in average pore diameter. The pore size distribution in the unreacted solid is relatively narrow, ranging from about 0.6 to 0.1 μm diameter, whereas in the partially hydrated solids, the distribution of pore sizes is wider and lies in the range of about 0.4 to 0.004 μm or less.

The pore structure in particles that rehydrate rapidly changes with hydration conversion in a different manner as illustrated in Figures 9 and 10 for anhydrous K_2CO_3 after one cycle and for dehydrated $K_2CO_3 \cdot 3/2H_2O$, respectively. The losses in total pore volume after 80% conversion are nearly the same for these two

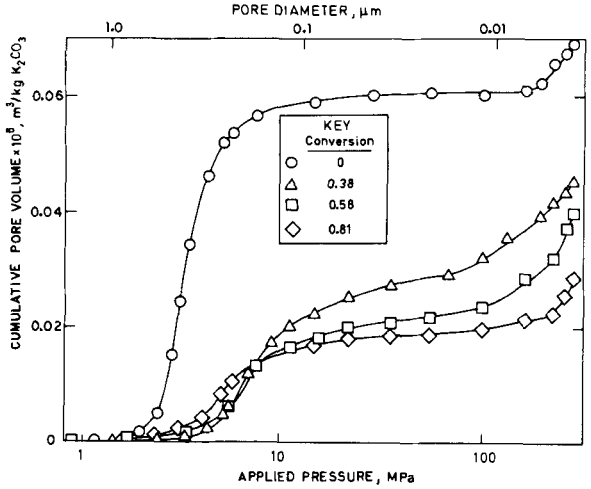

Figure 8. Pore volumes at different stages of the first hydration of 300–354 μm (−45 + 50 mesh) anhydrous K_2CO_3 particles (uncycled).

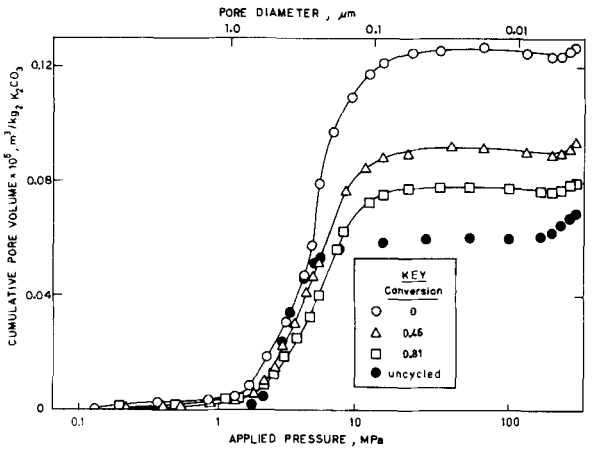

Figure 9. Pore volumes at different stages of the second hydration of K_2CO_3. Samples hydrated at T = 333 K, P = 2.3 kPa after one complete cycle of 300–354 μm (−45 + 50 mesh) anhydrous particles. Also shown for comparison are results for anhydrous sample as received before first cycle.

samples and for the uncycled anhydrous material. However, in these two samples, the initially narrow pore size distribution (0.6 to 0.09 μm, approximately) exhibits virtually no shift or spreading with hydration conversion.

From these porosimetry data, mean pore radii were calculated using the definition

$$r_e \equiv \frac{1}{(V_2 - V_1)} \int_{V_1}^{V_2} r dV \qquad (1)$$

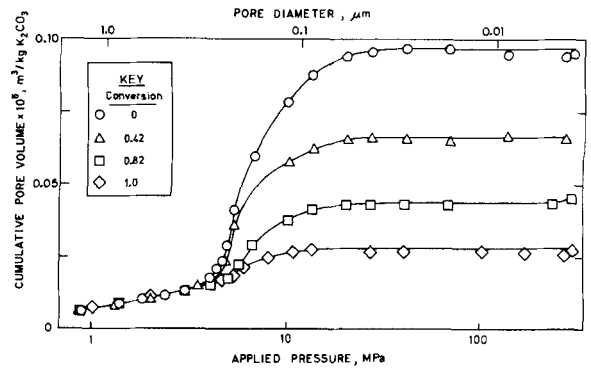

Figure 10. Pore volumes at different stages of the first hydration of K_2CO_3 prepared by dehydration 300–354 μm (−45 + 50 mesh) $K_2CO_3 \cdot 3/2H_2O$ particles at T = 343 K in vacuum.

and void fractions (ω) were calculated as the ratio of total pore volume to bulk solid volume. These results are presented in Table 2 and were used to estimate the listed effective Knudsen diffusivities via the expression of Satterfield (1980)

$$D = 97.0(\omega/\tau) r_e (T/M)^{1/2} \qquad (2)$$

where the tortuosity factor was assigned the value $\tau = 7$ (Stanish and Perlmutter, 1982). At less than 40% conversion, the estimated diffusivity in the uncycled anhydrous K_2CO_3 fell to less than 20% of its initial value. The declines in diffusivity for the other two more rapidly hydrating solids were significantly less steep. These results are qualitatively consistent with the observed hydration rate behavior presented in Figure 7(a), which shows that the rate of hydration of 300–354 μm particles of uncycled material should fall off rapidly near a conversion of about 0.2. In fact, if the pore shrinkage for uncycled K_2CO_3 were confined to an outer layer in those particles (a possibility which is neither proved nor disproved by the porosimetry data in Figure 8), the void fraction within that volume would be less than and the tortuosity greater than the corresponding values that were used in Eq. 2 to calculate the diffusivities listed in Table 2. In this case the diffusivities for partially hydrated uncycled K_2CO_3 shown in Table 2 would be over-estimated and it would appear even more likely that inhibited diffusion was responsible for the large decrease in hydration rate with conversion shown in Figure 7(a).

In a study of the reversible decomposition of Ag_2CO_3, Spencer and Topley (1931) reported increased recarbonization rates following each recarbonization-decomposition cycle. The low reactivity prior to cycling was attributed to a resistance to CO_2 diffusion in the sintered oxide; thus the increase in recarbonization rate after cycling was attributed to the formation of a cycled product with a loose physical structure. Although the water vapor-K_2CO_3 system may appear to be quite analogous, a close examination of the results presented here reveals more complicated behavior. For example,

TABLE 2. VARIATION OF PARTICLE DIFFUSIVITY WITH HYDRATION CONVERSION

Sample History		Conversion	Porosity	Mean Pore Radius	Diffus. Calc. via eq. 2
Form As Received	Prior Treatment	%	ω	r_e, μm	$D \times 10^6$, m²/s
Anhydrous K_2CO_3	None	0	0.12	0.21	1.5
		38	0.087	0.06	0.31
		58	0.074	—	—
		81	0.046	0.10	0.26
Anhydrous K_2CO_3	One Complete Cycle	0	0.23	0.22	3.1
		46	0.16	0.19	1.8
		81	0.13	0.21	1.6
$K_2CO_3 \cdot \frac{3}{2} H_2O$	Dehydrated Once	0	0.19	0.22	2.5
		42	0.12	0.26	1.9
		82	0.078	0.32	1.5
		100	0.041	—	—

changes in particle diffusivity do not explain the trends shown in Figure 6, in which earlier cycles exhibit greater degrees of induction and/or acceleration in the hydration conversion-time curve. In addition, a mechanism based solely on differences in diffusion coefficient provides no explanations for the similar manner of porosity change with conversion in rapidly hydrating solids, in spite of very different preparation history (Figures 9 and 10), nor for the quite different porosity change that occurs in a slowly hydrating specimen (Figure 8).

ACKNOWLEDGMENT

This research was supported by the U.S. Department of Energy through the Solar Energy Research Institute under Contract No. DE-FG02-80CS-84051-A002.

NOTATION

D = effective Knudsen diffusivity, m^2/s
M = molecular weight, kg/kmol
P = pressure, Pa
r = radius, m
r_e = effective mean pore radius, m
T = temperature, K
t = time, s
V = volume, m^3
X = conversion, dimensionless

Greek Letters

τ = tortuosity factor, dimensionless
ω = void fraction, dimensionless

Subscripts

eq = equilibrium

LITERATURE CITED

Ball, M. C., and L. S. Norwood, "Studies in the System Calcium Sulphate/Water: Part 4. Rehydration of Hexagonal $CaSO_4$," *J. Chem. Soc., Farad. Trans. I*, **69**, 169 (1973).

Bielanski, A., and F. C. Tompkins, "Sorption of Water by Dehydrated Alum Crystals," *Trans. Farad. Soc.*, **46**, 1072 (1950).

Eckhardt, R. C., P. M. Fichte, and T. B. Flanagan, "Kinetics of Rehydration of Crystalline Anhydrides-Manganous Formate," *Trans. Farad. Soc.*, **67**, 1143 (1971).

Eckhardt, R. C., and T. B. Flanagan, "Anisotropic Solid-State Reaction," *Trans. Farad. Soc.*, **60**, 1289 (1964).

Flanagan, T. B., "Dehydration Studies of Lead Styphnate Monohydrate," *Trans. Farad. Soc.*, **55**, 114 (1959).

Flanagan, T. B., "The Kinetics of Sorption and Desorption of Water Vapor by Lead Styphnate," *Can. J. Chem.*, **44**, 2941 (1966).

Grodzka, P. G., "Thermal Energy Storage," National Technical Information Service Report No. N76-13592 (Nov., 1975).

Hume, J., and J. Colvin, "The Dehydration of Copper Sulphate Pentahydrate," *Proc. R. Soc.*, **A132**, 548 (1932).

Satterfield, C. N., *Heterogeneous Catalysis*, McGraw-Hill New York (1980).

Spencer, W. D., and B. Topley, "Reaction Velocity in the System $Ag_2CO_3 \rightleftarrows Ag_2O + CO_2$," *Trans. Farad. Soc.*, **27**, 94 (1931).

Stanish, M. A., and D. D. Perlmutter, "Salt Hydrates as Absorbents in Heat Pump Cycles," *Solar Energy*, **26**(4), 333 (1981).

Stanish, M. A., and D. D. Perlmutter, "Kinetics and Transport Effects in the Dehydration of Crystalline Potassium Carbonate Hydrate," *AIChE J.* **29**, 806 (Nov., 1983).

Triollier, M., and B. Guilhot, "The Hydration of Calcium Sulphate Hemihydrate," *Cem. Concr. Res.*, **6**, 507 (1976).

Manuscript received May 27, 1982; revision received November 18, and accepted January 31, 1983.

Oxidative Absorption of H_2S and O_2 by Iron Chelate Solutions

Hydrogen sulfide is oxidized to elemental sulfur by ferric ion chelated with nitrilotriacetic acid (NTA) in aqueous solution at pH 3.5 to 4.5. The reaction appears to be fast relative to gas- and liquid-phase diffusion, and the transfer of H_2S from a gas stream is correlated well by the theory of absorption with instantaneous chemical reaction. The ferrous ion formed in this reaction may be reoxidized with oxygen absorbed from a stream of air. The presence of NTA catalyzes the reaction of O_2 and Fe^{2+} in the same pH range, and diffusion is again controlling. Design calculations based on laboratory data for both absorption steps show that cocurrent gas-liquid contactors are advantageous for achieving high reaction rates (e.g., ~99.99% H_2S removal), high gas velocities (10 to 20 m/s), low pressure drops [1 to 3 kPa (10 to 30 cm H_2O)], and moderate column heights (10 to 15 m).

D. W. NEUMANN and SCOTT LYNN

Department of Chemical Engineering
University of California
Berkeley, CA 94720

SCOPE

Hydrogen sulfide is a contaminant in many industrial gas streams that must be removed more or less completely for reasons of safety, environmental protection, and/or processibility. A number of processes have been introduced commercially that are based on the oxidative absorption of H_2S. In most cases the oxidizing agent is dissolved in an aqueous solution at pH 6 or higher. The desired action is to convert the H_2S to elemental sulfur while converting the oxidizing agent to a soluble reduced form that can be reoxidized with air. Ideally, both reactions should be effectively instantaneous. However, many of the